PERGAMON

International Journal of Heat and Mass Transfer 44 (2001) 2621–2631

International Journal of HEAT and MASS TRANSFER

www.elsevier.com/locate/ijhmt

An investigation of a block moving back and forth on a heat plate under a slot jet

Wu-Shung Fu *, Ke-Nan Wang, Wen-Wang Ke

Department of Mechanical Engineering, National Chiao Tung University, 1001 Ta Hsueh Road, Hsinchu 30056, Taiwan

Received 26 January 2000; received in revised form 21 September 2000

Abstract

An investigation of heat transfer rate of a heat plate under a slot jet was studied numerically. For enhancing the heat transfer rate of the heat plate, a block moves back and forth on the heat plate. Then the thermal boundary layer on the heat plate is destroyed by the moving block and a new thermal boundary layer reforms immediately as the block passes through. Consequently, the remarkable heat transfer enhancement of the heat plate is attained. This subject belongs to a kind of moving boundary problems, the modified arbitrary Lagrangian Eulerian (ALE) method is suitable for solving this subject. The results show that the maximum increment of heat transfer rate is about 200% in the largest velocity case.

1. Introduction

Up to now, numerous methods have been proposed to enhance heat transfer rate of a heat body. These methods which mainly include the passive methods such as treated surfaces, extended surfaces, swirl flow devices, and active methods such as surface vibration, fluid vibration, injection and suction were summarized and reviewed in detail by Bergles [1,2]. A jet impingement which has high heat transfer rate is one of the above active methods and widely used in the cooling apparatus for high heat flux system such as electric cooling and turbine blade cooling. However, accompanying with the progress of semiconductor technology, the smaller and more compact device is produced indefatigably. The heat generated by the new device is always several times of the former one and becomes the main defect of the failure of device. As a result, how to increase the heat transfer rate of the jet impingement becomes a very important issue.

In the past, Mujumdar and Douglas [3], Martin [4], and Jambunathan et al. [5] reviewed the contemporary literature. Marple et al. [6] used a flow visualization technique to study a confined water jet impingement and observed the laminar flow for jet Reynolds number up to 2300. Chou and Hung [7] studied fluid flow and heat transfers of a confined slot jet numerically and found that the Nusselt number at the stagnation line was proportional to jet Reynolds number in a 0.5 power and the ratio of separation distance to jet width in a −0.17 power. Chakroun et al. [8] investigated heat transfer of a round air jet impinging normally on a heated rough surface and found that the local and average Nusselt numbers of a rough surface were larger than those of a smooth surface by 8.9–28%. Chung et al. [9] investigated heat transfer characteristics of an axisymmetric jet impinging on a rib-roughened convex surface. The average Nusselt numbers on the rib-roughened convex surface were more than those on the smooth surface by 14–34%. Besides, in several experimental studies, an extra mechanism in the jet impingement system was installed to enhance the heat transfer rate of the jet impingement. Zumbrunnen and Aziz [10] investigated an intermittent water jet impinging on a constant heat flux surface experimentally, and found that the enhancement due to the intermittent flow only occurred as the frequency of the intermittence was sufficiently high enough. Haneda et al. [11] enhanced heat transfer rate of a jet impingement by inserting a suspended cylinder between the jet

* Corresponding author. Tel.: +886-3-5712121/5510; fax: 886-3-5720634.

E-mail address: wsfu@cc.nctu.edu.tw (W.-S. Fu).

0017-9310/01/$ - see front matter
PII: S0017-9310(00)00305-7

Nomenclature

b	dimensional width of the block (m)
h	dimensional height of the block (m)
H	dimensional height of the channel (m)
L	dimensional length of the channel (m)
n	normal vector of surface
Nu	Nusselt number
p	dimensional pressure (N m^{-2})
p_∞	dimensional reference pressure (N m^{-2})
P	dimensionless pressure
Pr	Prandtl number
Re	Reynolds number
t	dimensional time (s)
T	dimensional temperature (K)
u, v	dimensional velocities in x- and y-directions (m s^{-1})
U,V	dimensionless velocities in X- and Y-directions
W	dimensional width of slot (m)
x, y	dimensional Cartesian coordinates (m)
X, Y	dimensionless Cartesian coordinates

Greek symbols

α	thermal diffusivity (m^2 s^{-1})
δ	dimensional boundary layer thickness (m)
θ	dimensionless temperature
λ	penalty parameter
v	kinematic viscosity (m^2 s^{-1})
ρ	dimensional density (kg m^{-3})
τ	dimensionless time

Subscripts

0	airflow inlet
b	block
h	heat plate
j	jet
s	stagnation line
x	local

Superscripts

$-$	mean value
$\wedge$	grid

exit and the heat plate. The mechanically oscillatory motion of the cylinder vibrated the flow field, and the maximum Nusselt number around the stagnation point was augmented by about 20% compared to that without the insertion of a cylinder.

From the above literature, the increment of heat transfer rate of the jet impingement seems to have limitation in spite of installing any extra equipment. This could be the velocity and thermal boundary layers, which are disadvantageous to the heat transfer rate, are still on the heat plate. Consequently, as the huge enhancement of heat transfer rate is expected, the boundary layers mentioned above are necessarily destroyed.

Therefore, the aim of the study is to propose a new apparatus for increasing heat transfer rate of a heat plate under a jet impingement. This apparatus combines a thin block which moves back and forth along the heat plate under an impinging jet. As this apparatus is executed, the original boundary layers on the heat plate are destroyed by the moving block and the new ones reform right after. Then, based upon the reformation of the new boundary layers, the huge enhancement of the heat transfer rate of the heat plate can be attained.

The subject mentioned above belongs to a kind of moving boundary problems, and the arbitrary Lagrangian Eulerian (ALE) method modified by Fu and Yang [12] is suitably adopted to solve this problem. The results show that the boundary layer is destroyed as the block passes through and the new boundary layer reforms right after. Based upon the reformation of new boundary layer, the remarkable enhancement of heat transfer can be obtained.

2. Physical model

The physical model is shown in Fig. 1. A two-dimensional channel with length L and height H is used to simulate the confined air jet impingement system. The air, which maintains uniform velocity v_0 and low temperature T_0, respectively, flows into the channel from a slot BC with width W, and impinges normally on the heat plate FK with high temperature T_h. The heat plate is as wide as the slot jet. The other surfaces of the channel (surfaces AB, CD, EF and KL) are insulated. An insulated moving block GHIJ with height h and width b is set on the heat plate, and moves back and

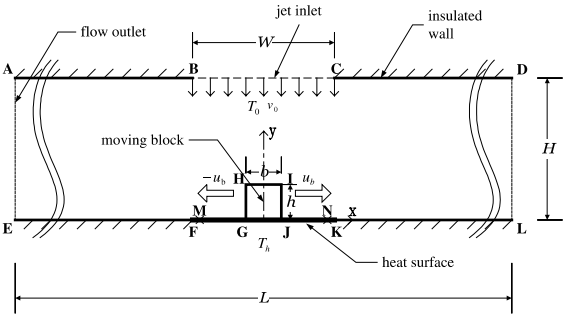

Fig. 1. Physical model.

forth from the positions M to N with a constant velocity u_b.

Initially ($t = 0$), the block is stationary at the middle position of the heat plate, and the flow field in the channel is steady. As time $t > 0$, the block starts to move along the MG line on the heat plate with the constant velocity $-u_b$. When the left surface GH of the block reaches the left point M, the block turns back instantly and moves to the right side with the constant velocity u_b. Similarly, when the right surface IJ of the block reaches the right point N, the block turns back immediately and moves to the left side with the constant velocity $-u_b$. The reciprocation motion of the block mentioned above is continuously executed on the region MN, then the original boundary layer on the heat plate is destroyed by the moving block and a new boundary layer reforms right after as the block passes through. Consequently, the behaviors of both the flow and thermal fields become time-dependent and can be categorized into a kind of moving boundary problems. As a result, the ALE method is properly utilized to analyze this problem.

For attaining the optimal heat transfer rate, the non-dimensional nozzle-to-plate spacing H/W was about 2.5 recommended by Chou and Hung [7]. Besides, in order to enhance the heat transfer rate effectively, the height of block must be greater than the thickness of the boundary layer so as to destroy the boundary layer completely. The non-dimensional boundary layer thickness (δ/W) is proportional to the jet Reynolds number in a 0.5 power and the non-dimensional nozzle-to-plate spacing in a 0.17 power [7]. As a result, when the jet Reynolds number is 100, the dimensionless thickness of boundary layer δ/W is about 0.24, the height of block is then determined as 0.3 W.

To simplify the analysis, the following assumptions and the dimensionless variables are made:

1. the flow field is two-dimensional and laminar,
2. the fluid is Newtonian and incompressible,
3. the fluid properties are constant,
4. the no-slip condition is held on the interface between the fluids and moving block,
5. the effect of gravity is neglected.

$$X = \frac{x}{W}, \quad Y = \frac{y}{W}, \quad U = \frac{u}{v_0}, \quad V = \frac{v}{v_0},$$
$$\hat{U} = \frac{\hat{u}}{v_0}, \quad U_b = \frac{u_b}{v_0}, \quad P = \frac{p - p_\infty}{\rho v_0^2}, \quad \tau = \frac{t v_0}{W}, \tag{1}$$
$$\theta = \frac{T - T_0}{T_h - T_0}, \quad Re_j = \frac{v_0 W}{\nu}, \quad Pr = \frac{\nu}{\alpha}.$$

Based upon the above assumptions and dimensionless variables, the dimensionless ALE governing Eqs. (2)–(5) are expressed as the following equations:

- continuity equation

$$\frac{\partial U}{\partial X} + \frac{\partial V}{\partial Y} = 0, \tag{2}$$

- momentum equations

$$\frac{\partial U}{\partial \tau} + (U - \hat{U})\frac{\partial U}{\partial X} + V\frac{\partial U}{\partial Y} = -\frac{\partial P}{\partial X} + \frac{1}{Re_j}\left(\frac{\partial^2 U}{\partial X^2} + \frac{\partial^2 U}{\partial Y^2}\right), \tag{3}$$

$$\frac{\partial V}{\partial \tau} + (U - \hat{U})\frac{\partial V}{\partial X} + V\frac{\partial V}{\partial Y} = -\frac{\partial P}{\partial Y} + \frac{1}{Re_j}\left(\frac{\partial^2 V}{\partial X^2} + \frac{\partial^2 V}{\partial Y^2}\right), \tag{4}$$

- energy equation

$$\frac{\partial \theta}{\partial \tau} + (U - \hat{U})\frac{\partial \theta}{\partial X} + V\frac{\partial \theta}{\partial Y} = \frac{1}{PrRe_j}\left(\frac{\partial^2 \theta}{\partial X^2} + \frac{\partial^2 \theta}{\partial Y^2}\right). \tag{5}$$

As $\tau > 0$, the boundary conditions are as follows:

- on the surfaces AB, CD, EF and KL

$$U = V = 0, \quad \partial\theta/\partial n = 0, \tag{6}$$

- on the inlet slot surface BC

$$U = 0, \quad V = -1, \quad \theta = 0, \tag{7}$$

- on the heat plates FG and JK

$$U = V = 0, \quad \theta = 1, \tag{8}$$

- on the outlet surfaces AE and DL

$$\partial U/\partial n = \partial V/\partial n = \partial\theta/\partial n = 0, \tag{9}$$

- on the surfaces of the block GH, HI and IJ

$$U = U_b, \quad V = 0, \quad \partial\theta/\partial n = 0. \tag{10}$$

3. Numerical method

A Galerkin finite element method with moving grids and a backward scheme dealing with the time differential terms are adopted to solve the governing equations (2)–(5). A penalty function and Newton–Raphson iteration algorithm are utilized to reduce the pressure and nonlinear terms in the momentum equations, respectively. The velocity and temperature terms are expressed as quadrilateral and nine-node quadratic isoparametric elements, and the degree of approximation for the penalty function terms are lower than those of the velocities terms for stability and convergence of the solution. The discretization processes of the governing equations are similar to those used in Fu and Yang [12]. Then, the momentum Eqs. (3) and (4) can be expressed as follows:

$$\sum_{1}^{n_e}\left([A]^{(e)}+[K]^{(e)}+\lambda[L]^{(e)}\right)\{q\}^{(e)}_{\tau+\Delta\tau}=\sum_{1}^{n_e}\{f\}^{(e)} \tag{11}$$

in which

$$(\{q\}^{(e)}_{\tau+\Delta\tau})^{\mathrm{T}}=\langle U_1,U_2,\ldots,U_9,V_1,V_2,\ldots V_9\rangle^{m+1}_{\tau+\Delta\tau}, \tag{12}$$

where $[A]^{(e)}$ includes the (m)th iteration values of U and V at time $\tau+\Delta\tau$; $[K]^{(e)}$ includes the shape function, $\hat{U}$ and time differential terms; $[L]^{(e)}$ includes the penalty function terms; $\{f\}^{(e)}$ includes the known values of U and V at time τ and (m)th iteration values of U and V at time $\tau+\Delta\tau$.

After the flow field is solved, the energy equation (5) can be expressed as follows:

$$\sum_{1}^{n_e}\left([M]^{(e)}+[Z]^{(e)}\right)\{c\}^{(e)}_{\tau+\Delta\tau}=\sum_{1}^{n_e}\{r\}^{(e)}, \tag{13}$$

where

$$(\{c\}^{(e)}_{\tau+\Delta\tau})^{\mathrm{T}}=\langle\theta_1,\theta_2,\ldots,\theta_9\rangle_{\tau+\Delta\tau} \tag{14}$$

in which $[M]^{(e)}$ includes the values of U and V at time $\tau+\Delta\tau$, $[Z]^{(e)}$ includes the shape function, $\hat{U}$ and time differential terms and $\{r\}^{(e)}$ includes the known values of θ at time τ. The value of penalty parameter used in the present study is 10^6 and the frontal method solver is utilized to solve Eqs. (11) and (13). The value of Prandtl number is 0.71 for air. The grid velocity $\hat{U}$ is linear distribution and inverse proportion to the distance between the nodes and the moving block.

A brief outline of the solution procedure are described as follows:

1. Determine the optimal grid distribution and number of the elements and the nodes.
2. Solve the values of the U, V and θ at the steady state and regard them as the initial values.
3. Determine the moving velocity U_b of the block, the time increment Δ_τ and the grid velocities $\hat{U}$ of every node.
4. Update the coordinates of the nodes and examine the determinant of the Jacobian transformation matrix to ensure the one-to-one mapping to be satisfied during the Gaussian quadrature numerical integration, otherwise execute the mesh reconstruction.
5. Solve Eqs. (11) and (13), until the following criteria for convergence are satisfied:

$$\left|\frac{\varphi^{m+1}-\varphi^{m}}{\varphi^{m+1}}\right|_{\tau+\Delta\tau}<10^{-3}, \tag{15}$$

where $\varphi=U,V$.

6. Continue the next time step calculation until the assigned time reaches.

For the thermal field, the energy balance is checked for every time step by the following equation:

$$E(\%)=\left(\int_{\mathrm{FK}}Nu_{\mathrm{x}}^{n+1}\,\mathrm{d}X-\int_{\mathrm{AE+DL}}Pr\cdot Re\cdot U^{n+1}\cdot\theta^{n+1}\,\mathrm{d}Y-\left(\left(Pr\cdot Re_j\cdot A\cdot\left(\bar{\theta}^{n+1}-\bar{\theta}^{n}\right)\right)\Big/\mathrm{d}\tau\right)\right)\Big/\left(\int_{\mathrm{FK}}Nu_{\mathrm{x}}^{n+1}\,\mathrm{d}X\right)\times 100, \tag{16}$$

where $\int_{\mathrm{FK}}Nu_{\mathrm{x}}^{n+1}\,\mathrm{d}X$ is the thermal energy added into the system from the heat plate, $\int_{\mathrm{AE+DL}}Pr\cdot Re_j\cdot U^{n+1}\cdot^{n+1}\mathrm{d}Y$ is the thermal energy leaving the system with the fluid and $(Pr\cdot Re_j\cdot A\cdot(\bar{\theta}^{n+1}-\bar{\theta}^{n}))/\mathrm{d}\tau$ is the increment of the internal energy.

The results of numerical tests of the non-dimensional time interval $\Delta\tau$ under $Re_j=100$ and $U_b=2$ are shown in Fig. 2. For economizing computational time, the value of non-dimensional time interval $\Delta\tau$ being equal to 5×10^{-3} is chosen. The computational meshes are tested by five different grids under $Re_j=100$ and $U_b=2$, and the variations of average Nusselt number are shown in Fig. 3. The local Nusselt number Nu_x and average Nusselt number $\bar{N}u_x$ are defined as the following equations:

$$Nu_{\mathrm{x}}=-\frac{\partial\theta}{\partial Y}|_{Y=0} \tag{17}$$

$$\bar{N}u_{\mathrm{x}}=\int_{\text{heat plate}}-\frac{\partial\theta}{\partial Y}|_{Y=0}\mathrm{d}X. \tag{18}$$

Based on the results, the grids 128×32 are chosen for computations. By the similar method, the other grids chosen for each case are shown in Table 1. The stagnation Nusselt number Nu_s is calculated without the block for the grid test. Chou and Hung [7] presented the stagnation Nusselt number as following equation:

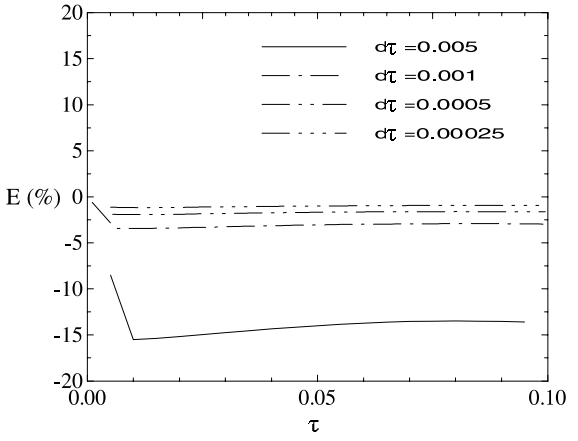

Fig. 2. The variations of the error of energy balance with τ under different time intervals $\mathrm{d}\tau$ for $Re_j=100$ and $U_b=2$ case.

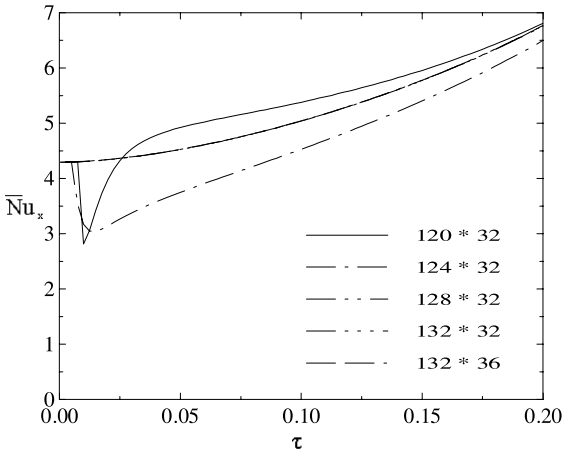

Fig. 3. The variations of the average Nusselt number $\bar{N}u_x$ with non-dimensional time under different grids for $Re_j = 100$ and $U_b = 2$ case.

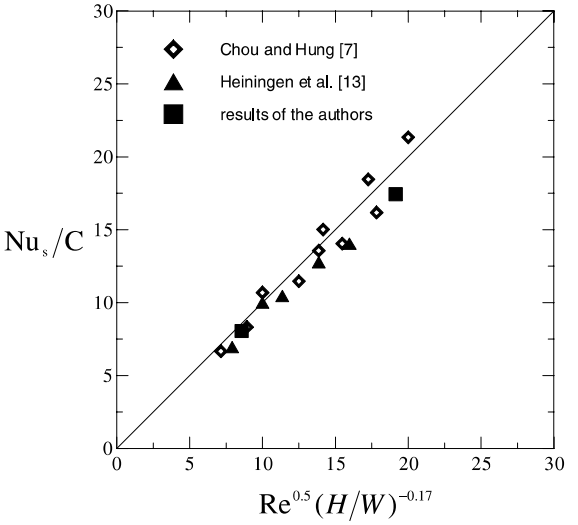

Fig. 4. Comparison of the results of the study with those of Chou and Hung [7] and Heiningen et al. [13].

$$Nu_s = CRe^{0.5}(H/W)^{-0.17}, \tag{19}$$

where C is 0.574 for the confined slot jet. Shown in Fig. 4, the stagnation Nusselt number calculated by the present study is consistent with the results of Chou and Hung [7] and Heiningen et al. [13].

4. Results and discussion

For clearly indicating the phenomena around the block, only the flow and thermal fields close to the moving block are illustrated in the following figures. The variations of the velocities, constant thermal lines and local Nusselt numbers Nu_x under $Re_j = 100$, and $U_b = 2.0$ are indicated in Figs. 5–7, respectively. These phenomena shown in Figs. 5–7 are in a certain period of total reciprocation motions.

In Fig. 5(a), the block is on the way moving to the left, and the position of block is at the center of the heat plate. The fluids before the moving block are pushed by the block and also flow to the left. The velocities of the fluids close to the moving block are much larger than those of the fluids far away from the moving block, which results in the original velocity boundary layer being destroyed by the moving block.

On the right surface of the block, the fluids complement the vacant space induced by the moving block instantly, and the directions of these fluids are left. As a result, a new velocity boundary layer reforms along the heat plate. The value of the velocities in the above new boundary layer are larger than those in the original boundary layer shown in the left side of the block apparently, and the increment of the velocities is beneficial to heat transfer rate. The stagnation point of the slot jet is not observed on the plate.

After the block passes the center of the heat plate, the block moves continuously to the left and the flow field is shown in Fig. 5(b). The variations of flow field are similar to those shown in Fig. 5(a). But the recirculation zone induced by the moving block becomes apparent. This could because of the addition of the fluids jetted by the left half of the slot jet.

The moving block reaches the left point M, and the flow field is shown in Fig. 5(c). The recirculation zone behind the moving block almost covers the heat plate.

Table 1
Grids and non-dimensional time intervals for each case

Case		Grids	Number of elements	Number of nodes	Non-dimensional time interval
Re	U_b				
100	1	128×32	4040	16,509	5×10^{-3}
	2	128×32	4040	16,509	5×10^{-3}
	4	132×32	4168	17,029	5×10^{-4}
500	1	154×32	4872	19,889	2×10^{-3}
	2	164×32	5192	21,189	5×10^{-3}

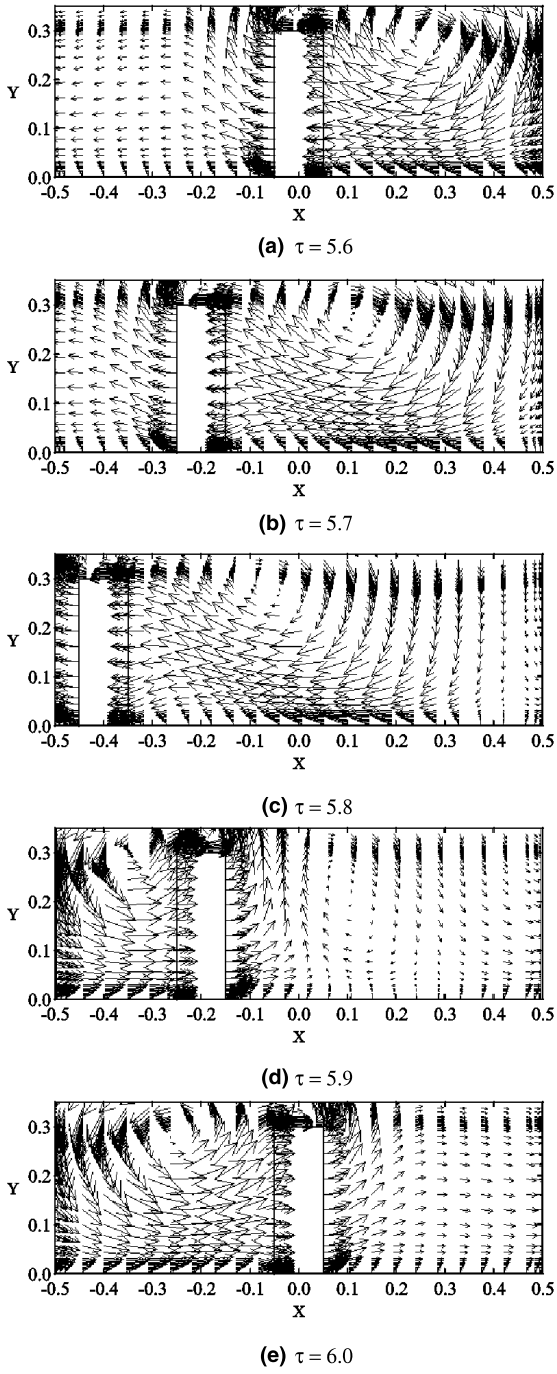

Fig. 5. The velocity vectors near the moving block for $Re_j = 100$ and $U_b = 2.0$ case.

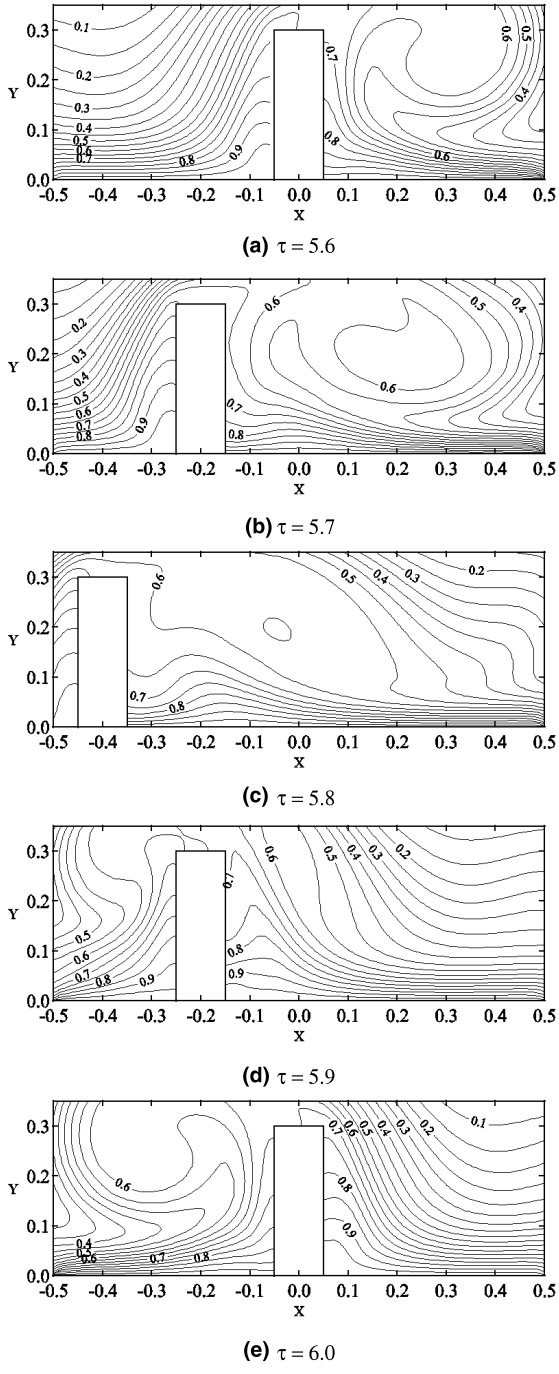

Fig. 6. The constant thermal lines near the moving block for $Re_j = 100$ and $U_b = 2.0$ case.

The part of fluids jetted by the right half of the slot jet impinge onto the heat plate and prevent the enlargement of the recirculation zone, and the stagnation region is then observed behind the recirculation zone.

The moving block turns back immediately, when the left surface of the block reaches the left point M. In Fig. 5(d), the block is on the way moving to the right. The moving block pushes the fluids near the right surface of

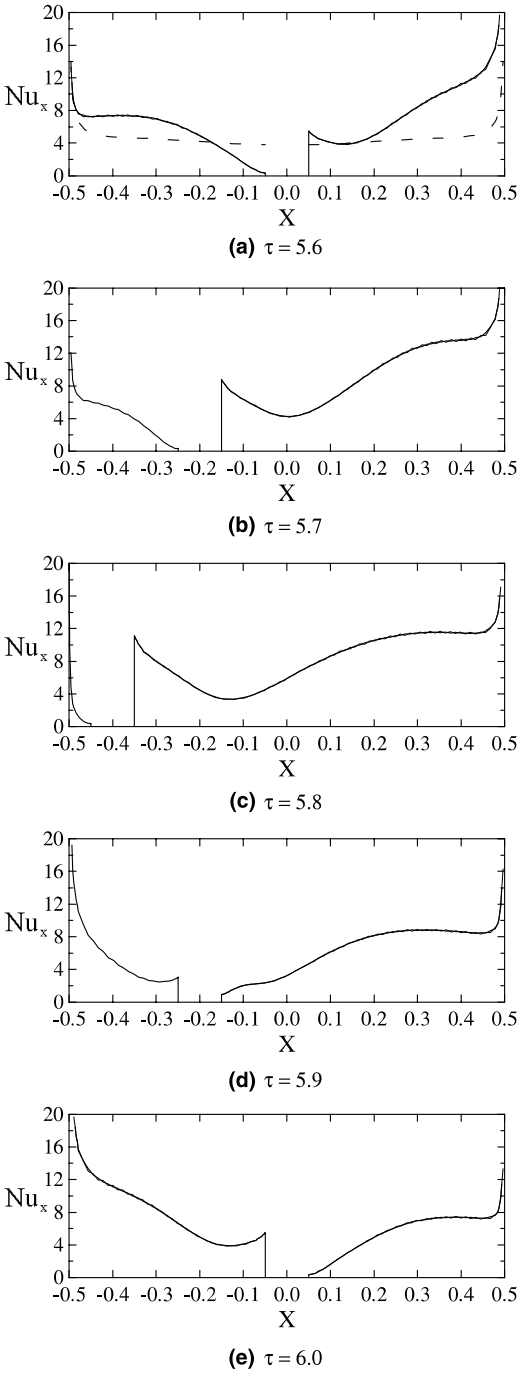

Fig. 7. The Nusselt number distributions on the heated surface for $Re_j = 100$ and $U_b = 2.0$ case.

the block to flow rightward. However, some fluids jetted by the left half side of the slot jet flow leftward. The two streams of the fluids mentioned above flow with different directions to interact with each other which causes the interflow to flow upward, and a small clockwise cell and a stagnation region are formed before the moving block. On the left side of the moving block, the fluids are induced by the moving block and a counterclockwise cell begins to be formed.

In Fig. 5(e), the block reaches the center of the heat plate again. Except the directions of the fluids, the structure of the flow field is similar to that shown in Fig. 5(a).

Figs. 6(a)–(e) show the distributions of constant thermal lines at the same condition shown in Figs. 5(a)–(e), respectively. The thermal fields represent the characteristics of the flow fields, and the thermal boundary layer on the heat plate is destroyed by the moving block and reforms right after as the moving block passes through. This results in the distributions of constant thermal lines near the front face of the moving block being spare; however, far away from the moving block the distributions of constant thermal lines are still dense. The new thermal boundary layer reforms after the moving block, the distributions of constant thermal lines are naturally dense which causes the heat transfer of the heat plate to be enhanced remarkably.

The distributions of local Nusselt number Nu_x are shown in the Figs. 7(a)–(e) at the same condition shown in Figs. 6(a)–(e), respectively. The dash line shown in Fig. 7(a) indicates the distributions of the local Nusselt number of the heat plate when the block is stationary on the center of the heat plate. The solid lines indicate the distributions of the local Nusselt number of the heat plate as the block is moving. Due to the insulation of the block, the distributions of local Nusselt number shown in these figures are interrupted. The moving block pushes the fluids near the front surface of moving block directly, and causes the local Nusselt number to become extremely small. Oppositely, the thermal boundary layer reforms behind the moving block which leads the local Nusselt number to become large apparently. Far away from the moving block, the fluids induced by the moving block flow toward the heat plate that is beneficial to the heat transfer rate of heat plate. Consequently, the distributions of local Nusselt number of the case for the block being moving become larger than those of the case for the block being stationary.

The variations of the average Nusselt number $\bar{N}u_x$ of the heat plate obtained by the block moving reciprocally on the heat plate several times are shown in Fig. 8. The conditions of the points a, b, c, d and e are the same as those figures mention above. As the block moves to the left shown in Figs. 5(a) and (b), the new thermal boundary layer reforms right after the moving block and the recirculation zone behind the moving block induces more low temperature fluids to flow toward the heat plate which causes the average Nusselt number to increase continuously (the curve ab in Fig. 8). However, when most impingement region of the jet is occupied by

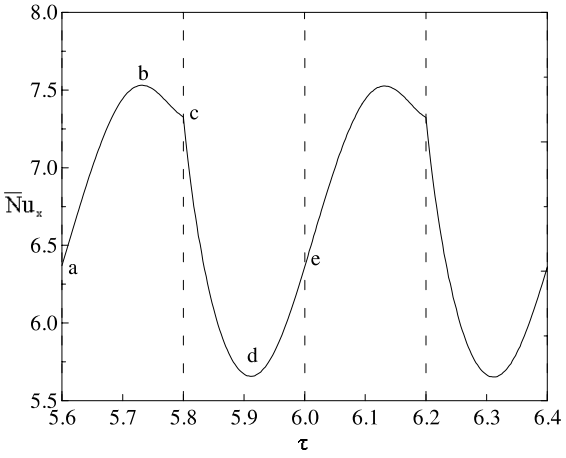

Fig. 8. The variations of the average Nusselt number $\bar{N}u_x$ during the τ to 6.4 for $Re_j = 100$ and $U_b = 2.0$ case.

the recirculation zone behind the moving block shown in Figs. 5(b) and (c), the jet flow prevents the formation of the recirculation zone which means the low temperature fluids to be difficultly induced by the recirculation zone and to flow difficultly toward the heat plate. The average Nusselt number then decreases before the moving block reaches the left point M (the curve bc in Fig. 8).

As the block moves rightward form the left point M (Fig. 5(d)), the local Nusselt number decreases before the block, and the increment of local Nusselt number behind the block is small because the new thermal boundary layer reforms in the wake of the moving block. Then, the average Nusselt number decreases continuously (curve cd in Fig. 8). When the block approaches the center of the heat plate (Fig. 5(e)), the recirculation zone behind the block enlarges gradually, and more chill fluids induced by the recirculation zone flow toward the heat plate again. The average Nusselt number then begins to increase (curve de in Fig. 8). As the block passes through the center of the heat plate and moves continuously to the right, the behaviors of the flow and thermal fields are similar to those of the block moving leftward at the same position. Then the variations of the average Nusselt number become periodic.

The velocity vectors for different block moving velocities U_b under $Re_j = 100$ are shown in Fig. 9. As the block is at the center of heat plate and moves to the left, the fluids near the upper front surface of the block flow upward, and a recirculation zone is formed behind the block. As the upward fluids flow over the block, the flow of fluids is divided into two flows as the rightward and leftward flows, and a stagnation region is formed. The stagnation region prevents the fluids jetted by the jet to impinge on the heat plate before the block. With the increment of the moving velocity U_b, the upward fluids flow rightward by the inducement of the recirculation

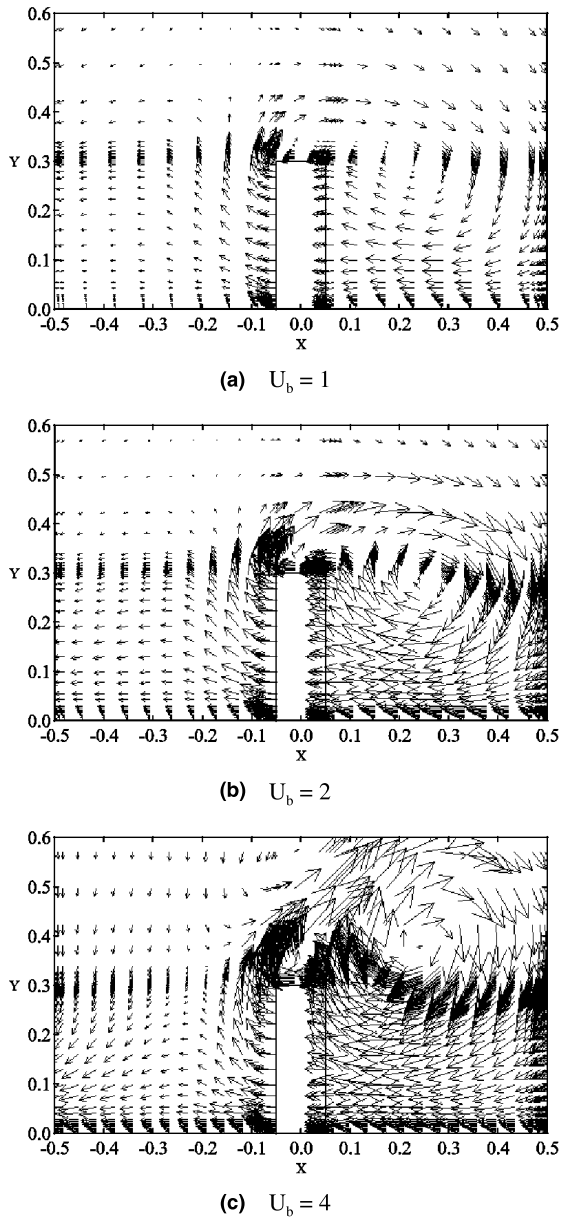

Fig. 9. The velocity vectors near the moving block for different moving velocities of the block for $Re_j = 100$ case.

zone behind the block. Then, the stagnation region mentioned above does not form and the fluids jetted by the jet can impinge onto the heat plate. As a result, the heat transfer rate becomes extremely large far away before the block.

Fig. 10 illustrates the constant thermal lines under the same condition shown in Fig. 9. With the increment of the moving velocity of block, the thermal boundary layer on the heat plate becomes thinner, which results in

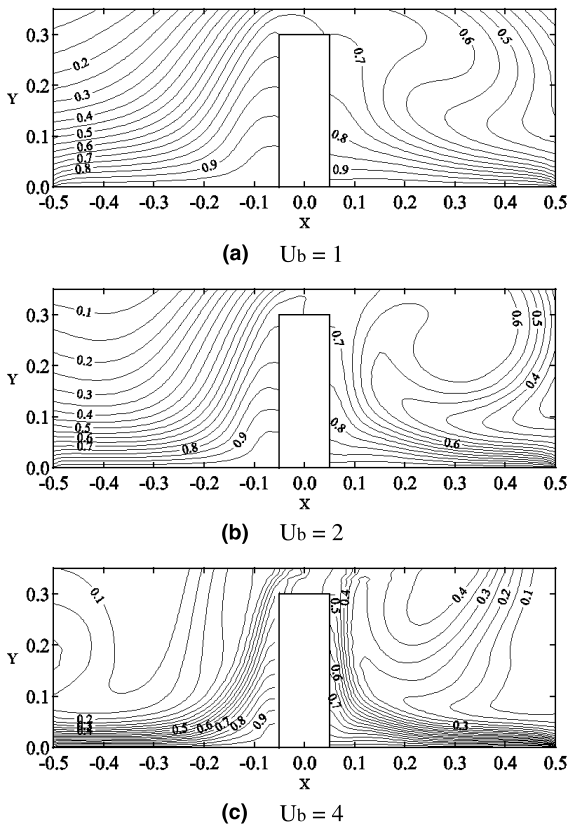

Fig. 10. The constant thermal lines near the moving block for different moving velocities of the block for $Re_j = 100$ case.

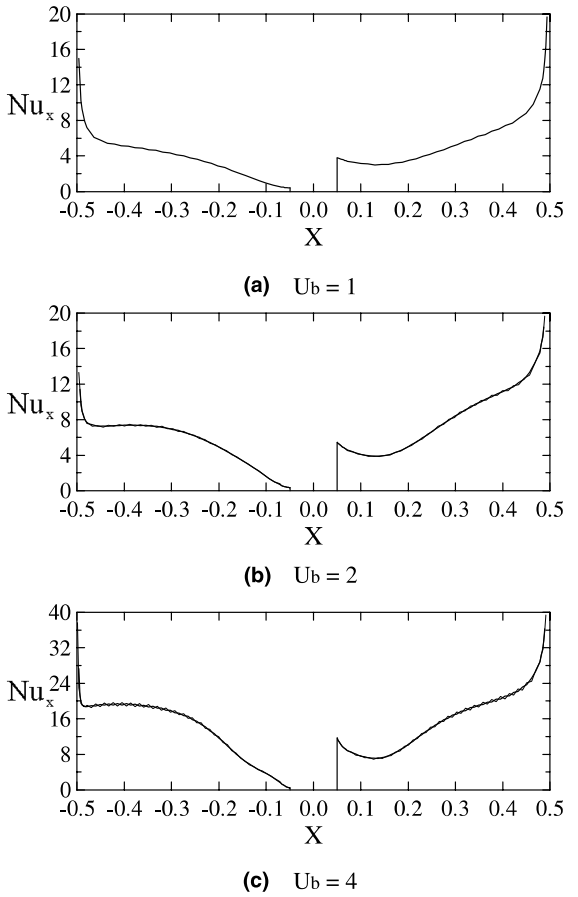

Fig. 11. The distributions of local Nusselt numbers on the heated surface for different block moving velocities for $Re_j = 100$ case.

the distribution of the constant thermal lines becoming denser for the large moving velocity.

The distributions of local Nusselt numbers Nu_x are shown in Fig. 11 under the same condition shown in Fig. 10. The distributions of the local Nusselt number under different block moving velocities are similar. Based upon the reason mentioned above, the larger the moving velocity is, the larger the local Nusselt number is attained.

Figs. 12–14 show the variations of average Nusselt numbers per unit cycle $\bar{N}u$ on the heat plate with the moving velocity of block being equal to 1.0, 2.0, and 4.0, respectively. The average Nusselt number per unit cycle is defined as following equation:

$$\bar{N}u = \frac{1}{m}\sum_{i=1}^{m}\left(\int_{\text{heat plate}} Nu_x \, dX\right)_i, \tag{20}$$

where m is the number of the time steps per unit cycle.

The sign "◆" shown in these figures indicate the average Nusselt number per unit cycle $\bar{N}u$, and the dash lines represent the average Nusselt number of the heat plate under the same condition when the block is stationary on the center of the heat plate.

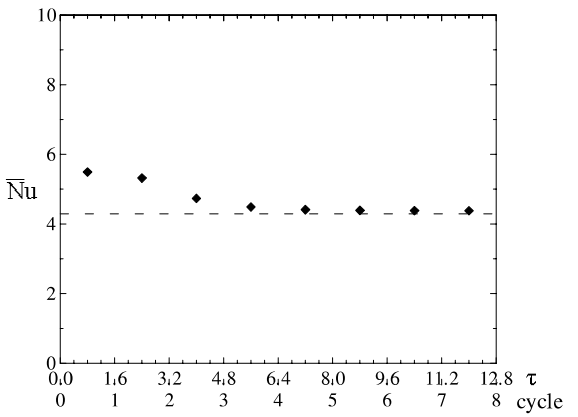

Fig. 12. The variations of average Nusselt number per unit cycle $\bar{N}u$ with τ for $Re_j = 100$ and $U_b = 1.0$ case.

As shown in Fig. 12, the heat transfer rate is enhanced by the moving block in the first three cycles. After that the enhancement of heat transfer rate is hardly observed.

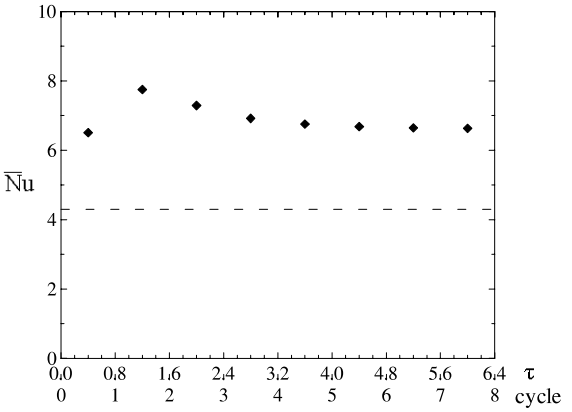

Fig. 13. The variations of average Nusselt number per unit cycle $\bar{N}u$ with τ for $Re_j = 100$ and $U_b = 2.0$ case.

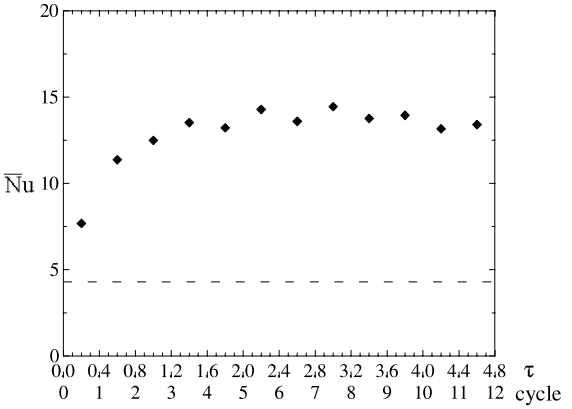

Fig. 14. The variations of average Nusselt number per unit cycle $\bar{N}u$ with τ for $Re_j = 100$ and $U_b = 4.0$ case.

In the total duration, the magnitude of enhancement of total heat transfer rate is small and about 2%, this could be the moving velocity of the block to be small and not to affect the fluids jetted by the slot jet.

Fig. 13 shows the variations of average Nusselt number per unit cycle $\bar{N}u$ when the moving velocity of block is 2.0. The moving velocity of block is higher enough to destroy the original thermal boundary layer and a new thermal boundary layer reforms. Then the increment of the total Nusselt numbers becomes larger and is about 54.46% in this duration.

In Fig. 14, the block moves with the velocity $U_b = 4.0$. The variations of the average Nusselt number per unit cycle are not periodic, this is suggested as that the moving velocity of block is too fast and the flow and thermal fields do not develop to the stable state. The enhancement of heat transfer rate is about 220%.

5. Conclusions

A numerical investigation of heat transfer of a block moving back and forth on a heat plate under a slot jet is studied. The main conclusions can be summarized as follows:

- The modified Arbitrary Lagrangian Eulerian method is suitable for solving the moving boundary problem.
- The thermal boundary layer on the heat plate is destroyed by the moving block and reforms right after as the block passes through. The reformation of the thermal boundary layer is the main mechanism for enhancing heat transfer of the heat plate.
- The factors of the moving velocity and position of the block affect the heat transfer of heat plate.

Acknowledgements

The support of this work by National Science Council, Taiwan, ROC under contract 89-2212-E-009-072 is gratefully acknowledged.

References

[1] A.E. Bergles, Recent development in convective heat-transfer augmentation, Appl. Mech. Rev. 26 (1973) 675–682.
[2] A.E. Bergles, Survey and evaluation of techniques to augment convective heat and mass transfer, Progr. Heat Mass Transfer 1 (1969) 331–424.
[3] A.S. Mujumdar, W.J.M. Douglas, Impingement heat transfer: a literature survey, TAPPI Meeting, SM 8603.7, NO, 1972, pp.107–136.
[4] H. Martin, Heat and mass transfer between impinging gas jets and solid surfaces, in: T. Irvine, J.P. Harnett (Eds.), Advances in Heat Transfer, vol. 13, Academic Press, New York, 1977, pp. 1–60.
[5] K. Jambunathan, E. Lai, M.A. Moss, B.L. Button, A review of heat transfer data for single circular jet impingement, Int. J. Heat Mass Transfer 13 (2) (1992) 106–115.
[6] V.A. Marple, B.Y.H. Liu, K.T. Whitby, On the flow fields of inertial impactors, J. Fluids Eng. Trans. ASME. 96 (1974) 394–400.
[7] Y.J. Chou, Y.H. Hung, Impingement cooling of an isothermally heated surface with a confined slot jet, ASME. J. Heat Transfer 116 (1994) 479–482.
[8] W.M. Chakroun, A.A. Abdel-Rahman, S.F. Al-Fahed, Heat transfer augmentation for air jet impinged on a rough surface, Appl. Thermal Eng. 18 (1998) 1225–1241.
[9] Y.S. Chung, D.H. Lee, J.S. Lee, Heat transfer characteristics of an axisymmetric jet impinging on the rib-roughened convex surface, Int. J. Heat Mass Transfer 42 (1999) 2101–2110.
[10] D.A. Zumbrunnen, M. Aziz, Convective heat transfer enhancement due to intermittency in an impinging jet, ASME. J. Heat Transfer 115 (1993) 91–98.

[11] Y. Haneda, Y. Tsuchiya, K. Nakabe, K. Suzuki, Enhancement of impinging jet heat transfer by making use of mechano-fluid interactive flow oscillation, Int. J. Heat Fluid Flow 19 (1998) 115–124.

[12] W.S. Fu, S.J. Yang, Numerical simulation of heat transfer induced by a body moving in the same direction as flowing fluids, Heat Mass Transfer 36 (2000) 257–264.

[13] A.R.P. van Heiningen, A.S. Mujumdar, W.J.M. Douglas, Numerical prediction of the flow field and impingement heat transfer caused by a laminar slot jet, ASME. J. Heat Transfer 98 (1976) 654–658.